

Microfluidic in-reservoir pre-concentration using a buffer drain technique†

Cite this: *Lab Chip*, 2014, 14, 2778

Received 6th March 2014,
Accepted 8th May 2014

DOI: 10.1039/c4lc00289j

www.rsc.org/loc

Junghyo Yoon,^a Youngkyu Cho,^a Sewoon Han,^a Chae Seung Lim,^b
Jeong Hoon Lee^c and Seok Chung^{*a}

Pre-concentration methods are essential for detecting low concentrations of influenza virus in biological samples from patients. Here, we describe a new method for draining buffer from solution in the reservoir of a microfluidic device to increase the concentration of virus in the reservoir. Viruses were captured in the reservoir by an ion depletion barrier from connected ion selective microfluidic channels. 75 μL of buffer was successfully drained from a 100 μL sample, resulting in a 4-fold increase in influenza hemagglutinin concentration in the reservoir. The volume of the final concentrated sample was suitable for detection of influenza hemagglutinin by the enzyme-linked immunosorbent assay, demonstrating the usefulness of the developed platform for enhanced sensitivity of virus detection in a conventional analysis.

The importance of detecting low concentrations of molecules in biological samples in a variety of assays has spurred the rapid development of pre-concentration techniques. Since biomarker proteins related to cancer and other diseases are often present at very low concentrations, a major challenge for biosensing is enhancing the detection sensitivity for highly diluted analytes. Therefore, pre-concentration of proteins could provide a powerful tool, especially for application in microfluidic-based miniaturized systems. Capillary electrophoresis,¹ isoelectric focusing,² isotachopheresis,³ membrane filtration,⁴ and ion concentration polarization (ICP) with ion-selective membranes^{5–8} have been integrated into microfluidic devices as a means to rapidly and selectively enrich target molecules.

Considerable research effort has been devoted in developing the ion-selective membrane technique using ICP, and these studies have demonstrated the feasibility of this approach in various applications. However, most of these efforts are focused on collecting a small amount of sample in the middle of a microfluidic channel;^{6–8} consequently, extraction of the concentrated sample is a major hurdle for the application of subsequent analyses, including rapid kit assay, enzyme-linked immunosorbent assay (ELISA), quantitative reverse transcription-polymerase chain reaction (qRT-PCR), and matrix-assisted laser desorption/ionization time-of-flight mass spectrometry (MALDI-TOF). Generally the analyses need a relatively large amount of concentrated sample volume of several tens of microns, compensating for pipetting error and acquiring statistical significance.^{9,10} Among the key hurdles in the practical application of this approach are the small amount of the sample in the microfluidic channel (<1 μL) and the dispersion and diffusion of the concentrated plug. To use the concentrated sample in the commercial analysis tools, researchers must overcome problems associated with moving the pre-concentrated plug into the analyzers.

In this paper, we propose a new method for concentrating virus directly in a reservoir using an ion-depletion barrier. In this system, neutral ions and buffer are drained by pressure-driven flow, resulting in the concentration of charged molecules in the reservoir. A schematic of the developed device is illustrated in Fig. 1a. The device was designed to contain two reservoirs connected *via* a microfluidic channel, 50 μm high by 1000 μm wide. The sample is placed in the right reservoir (red), and buffer is drained from the left reservoir (blue) by a syringe pump. The inside of the microfluidic channel was coated with an ion-permselective membrane (Nafion). The basic concept behind collecting the pre-concentrated sample in the sample reservoir is simple: charged molecules are blocked from the drain in front of the Nafion-coated microfluidic channel through application of an electric field, while buffer is drained by pressure-driven flow.

^a School of Mechanical Engineering, Korea University, Seongbuk, Seoul 136-701, Korea. E-mail: sidchung@korea.ac.kr

^b Department of Laboratory Medicine, College of Medicine, Korea University, Seongbuk, Seoul 136-701, Korea

^c Department of Electrical Engineering, Kwangwoon University, Nowon, Seoul, 139-701, Korea

† Electronic supplementary information (ESI) available: Details of bubble generation by electrolysis, chip fabrication, activating conditions for the three phases, force comparison, and values for the remaining sample volume and the concentration of the sample. See DOI: 10.1039/c4lc00289j

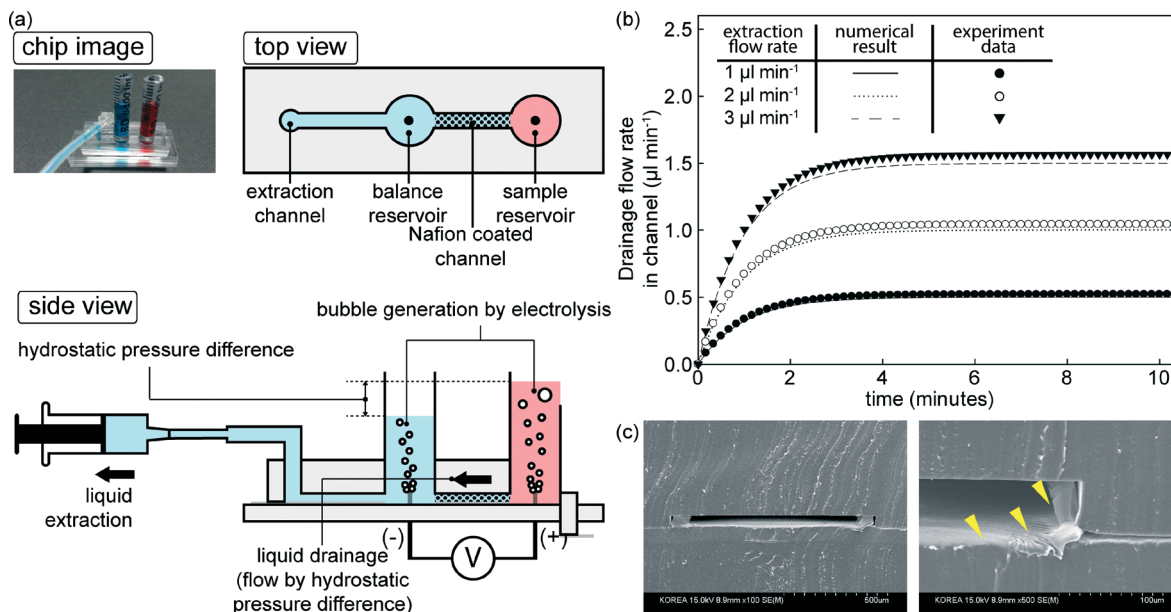


Fig. 1 (a) Picture and schematic view of the developed device. Two reservoirs were used to stably drain buffer while eliminating the bubbles generated around the electrodes. (b) Measured drain flow rates at various syringe pump extraction flow rates were strongly correlated with numerical estimates. (c) Scanning electron microscopy images of the Nafion-coated microfluidic channel (yellow arrowheads indicate the parts coated with Nafion).

Application of an electric field to electrodes in the reservoirs produces bubbles around the electrodes by electrolysis at a rate of up to several microliters per minute (Fig. S1,† calculated by Faraday's Second Law of Electrolysis). The effect of generated bubbles is eliminated by balancing the hydrostatic pressure between the sample and balance reservoirs, both of which are open to the atmosphere. Liquid extraction from the balance reservoir by the syringe pump reduces hydrostatic pressure in the balance reservoir, and the pressure difference (ΔP) between the two reservoirs generates drain from the sample reservoir through the Nafion-coated microfluidic channel. The flow rate of the drain from the sample reservoir was calculated using the Poiseuille equation, $\Delta P = 128 \mu L Q \pi^{-1} d^{-4}$, where μ is the dynamic viscosity of the solution, L is the length of the Nafion-coated channel, Q is the flow rate through the Nafion-coated channel, d is the diameter of the reservoirs, and $Re \ll 1$. The calculated drain rate from the sample reservoir was half of that of the liquid-extraction flow rate applied by the syringe pump, a value that was strongly correlated with experimental results (Fig. 1b).

Fig. S2a† shows the method for fabricating the device and coating the PDMS (polydimethylsiloxane, Sylgard 184; Dow Chemical, MI, USA) microfluidic channel with Nafion. A 2 μl solution of 10% Nafion (Sigma-Aldrich, St. Louis, MO) in isopropanol was injected into the bonded microfluidic channel from the right reservoir, and the reservoir was then covered by a glass coverslip (Fig. S2i†). Isopropanol was then evaporated by placing the Nafion-filled device on a hot plate at 60 °C (Fig. S2ii†). During evaporation, gas in the covered reservoir expanded and flowed out into the left reservoir, creating a

large hole in the filled Nafion; the resulting dried Nafion coated the inside of the microfluidic channel. The bottom of the PDMS membrane was punched to remove Nafion remaining in the reservoirs (Fig. S2iii†), and another bare PDMS plate was bonded to the bottom of the PDMS membrane (Fig. S2iv†). Leaving the reservoir uncovered during evaporation causes the remaining Nafion solution to block the microfluidic channel (Fig. S2b†). Scanning electron microscopy images of a Nafion-coated microfluidic channel are shown in Fig. 1c.

The formation of an ion-depletion region during liquid extraction by the syringe pump and electric field application was found to consist of three phases: (i) drag, (ii) focusing, and (iii) depletion-barrier. Fig. 2 shows a schematic depiction of the movement of particles and ions and the distribution of fluorescent microsphere tracers ($0.2 \mu\text{g ml}^{-1}$, 100 nm diameter; Invitrogen, Carlsbad, CA, USA) in each phase at -3.65 mV in $0.1\times$ phosphate-buffered saline (PBS). The activating conditions of each phase with respect to applied electric fields and extraction flow rates are presented in Fig. S3.† The motion of particles in the phases involved a total force (F) comprising three individual forces: hydrodynamic drag (F_D), electrophoretic (F_{EP}) and depletion by ICP (F_{ICP}), where $\sum F = F_D + F_{EP} + F_{ICP}$.^{6,11,12} F_D , following Stokes' law under a low Reynolds flow, made particles follow the direction of the flow, whereas F_{EP} acted in the direction of the electric field. F_{ICP} repelled the particles from the Nafion-coated channel surface. The lift force toward the center line through an inertia effect owing to differences in density between the particle and fluid was negligible because of the relatively short channel length ($\sim 5 \text{ mm}$).¹³

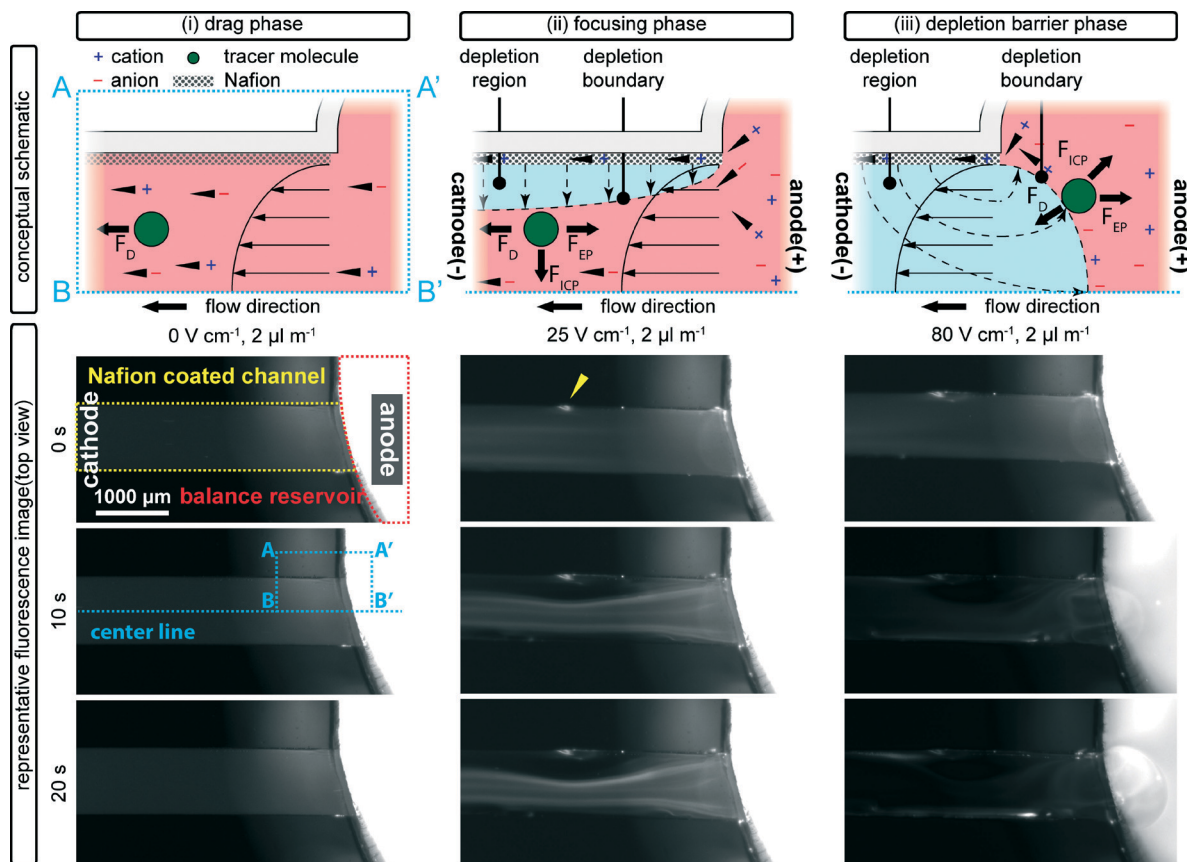


Fig. 2 Three phases of particle movement under applied electric fields and drain flow: (i) drag, (ii) focusing, and (iii) depletion barrier. Parabolic solid lines and solid arrows indicate the flow profile in the Nafion-coated channel. Dashed lines and dashed arrows indicate the boundary of the depletion region and the direction of the depletion force, respectively. Black arrowheads indicate the movement of ions. Fluorescence images show the distribution of tracers in the three stages. Blue dotted rectangles and blue dotted lines represent the position of the conceptual schematic image and the center of the microfluidic channel, respectively. The yellow arrowhead indicates accumulated fluorescent particles.

In the drag phase, prior to application of the electric field, tracers in the Nafion-coated channel were evenly distributed with drain flow (Fig. 2i and region A in Fig. S3†). All components in the liquid solution (anions, cations, and tracer molecules) moved into the direction of the flow, maintaining electro-neutrality. In the focusing phase (Fig. 2ii and region B in Fig. S3†), with application of both electric field and drain flow, tracers were focused toward the center of the Nafion-coated microfluidic channel. Immediately after application of the electric field, cations in solution started to migrate through the Nafion onto the microfluidic channel surface because the electric resistance (at 25 °C) of Nafion ($3.65 \times 10^5 \text{ S}^{-1}$) is much lower than that of the liquid ($5.4 \times 10^{10} \text{ S}^{-1}$), as previously reported.¹⁴ This resulted in the formation of a center-directional gradient of F_{ICP} and the development of a partially depleted region near the Nafion surface. Focused flow was symmetric but easily interrupted by accumulated fluorescent particles in the side corners (yellow arrowhead in Fig. 2). A stronger electric field increased F_{ICP} and the ion-depletion area, marking the beginning of the depletion-barrier phase (Fig. 2iii and region C in Fig. S3†). The ion-depletion region wholly overtook the inside of the Nafion-coated microfluidic channel, blocking anions and tracer molecules from passing

through the channel. In the depletion-barrier phase, F_{D} and F_{ICP} dominated the motion of charged ions and molecules (see Table S1† for details).

The area of the depletion barrier was determined from the applied electric field and the drain flow rate. Fig. 3a shows the growth and stabilization of the ion-depletion barrier in the sample reservoir in an electric field of 80 V cm^{-1} and at a syringe extraction flow rate of $2 \mu\text{l min}^{-1}$ (drain flow rate, $1 \mu\text{l min}^{-1}$). During the first few seconds, tracers, which were initially distributed evenly in the Nafion-coated microfluidic channel, accumulated at the anode side with the vortex, and the area of the depletion barrier gradually increased. At 1 minute, the depletion barrier started to decrease because the supply of cations to Nafion by the developing drain flow was less than the electromigration of cations through Nafion (Fig. 3a and b). Once fully developed, drain flow stabilized the depletion barrier for up to 15 minutes. At all syringe flow rates, the depletion barrier under a stronger electric field (80 V cm^{-1}) was larger than that under a weaker electric field (60 V cm^{-1}), owing to increased electromigration of cations. Drain flow helped rapidly (≤ 1 minute) stabilize the ion-depletion barrier by increasing F_{D} and supplying cations to the Nafion membrane. Even at a high extraction flow rate of

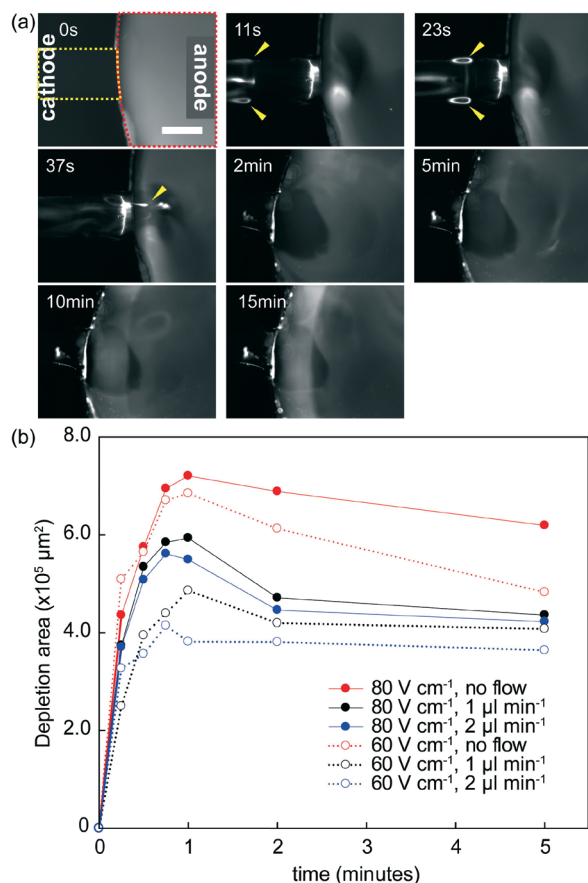


Fig. 3 (a) Tracers showing depletion-barrier development in an electric field of 80 V cm^{-1} and an extraction flow rate of $2 \mu\text{l min}^{-1}$. Yellow and red dashed lines indicate the positions of the Nafion-coated microfluidic channel and the sample reservoir, respectively, and yellow arrowheads indicate vortices. Scale bar, $500 \mu\text{m}$. (b) Projection area of the ion-depletion barrier.

$2 \mu\text{l min}^{-1}$, the depletion barrier was successfully maintained for more than 15 minutes; however, a higher drain flow rate prevented the stable formation of an ion-depletion barrier.

To assess the utility of this system as a bioassay platform, we tested its ability to concentrate a dilute sample of influenza hemagglutinin, one of the influenza A virus membrane proteins responsible for binding the virus to cells.¹⁵ The sample reservoir was filled with a $100 \mu\text{l}$ sample of recombinant hemagglutinin mixed with $0.1\times$ PBS buffer, and the balance reservoir and Nafion-coated microfluidic channels were filled with buffer. In this application, we used a modified version of our microfluidic device in which the sample and balance reservoirs were connected with five Nafion coated channels to achieve a high extraction flow rate of $10 \mu\text{l min}^{-1}$ (drain flow rate, $5 \mu\text{l min}^{-1}$) from the sample reservoir (Fig. 4a). The concentration of hemagglutinin in the sample reservoir was verified using a conventional ELISA kit (H1N1, Swine Flu 2009 Hemagglutinin ELISA kit; Sino Biological Inc., China). The initial concentration of hemagglutinin in the sample reservoir was 334 pg ml^{-1} . After draining for 15 minutes, $75 \mu\text{l}$ of buffer was removed, leaving a more concentrated sample

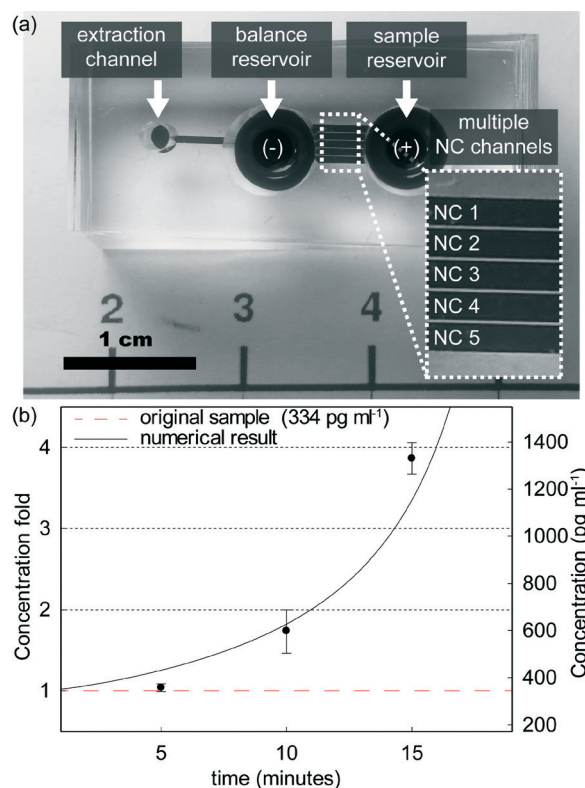


Fig. 4 (a) Modified device with two reservoirs connected by five Nafion-coated microfluidic channels (NC 1 to 5). (b) Fold increase in concentrations measured by ELISA after pre-concentration for 5, 10 and 15 minutes ($n = 4$; error bars indicate standard error).

of hemagglutinin in a volume of $25 \mu\text{l}$, a volume suitable for subsequent analysis using conventional tools, such as ELISA, qRT-PCR, or other rapid analytical tests (see Table S2†). As shown in Fig. 4b, ELISA measurements confirm that the sample was concentrated ~ 1.7 -fold in 10 minutes (average, 598 pg ml^{-1}) and 3.9 -fold in 15 minutes (average, 1329 pg ml^{-1}). Thus, in 15 minutes, $100 \mu\text{l}$ of the sample was reduced to $25 \mu\text{l}$, a 4-fold difference, with only 3.5% loss of the sample. The pre-concentration ratio is determined by the ratio of the initial sample volume and the final target volume, and the time required can be reduced by increasing the number of Nafion-coated microfluidic channels.

In conclusion, we have developed a new method for pre-concentration of biological samples based on the formation of an ion-depletion barrier by Nafion-coated microfluidic channels. Applying this platform to pre-concentrate recombinant H1N1 hemagglutinin, we achieved an approximately 4-fold increase in concentration in 15 minutes with only 3.5% loss of protein, yielding a volume of the sample sufficient for ELISA quantification. The 4-fold increase is not a dramatic enhancement but could be useful to enhance sensitivity of analytical virus detection, as reported in ref. 16. Various application fields including rapid kits will be explored in the future study. This new method is free from bubbles generated by electrolysis and enables direct integration of the microfluidic function of pre-concentration with conventional

analytical tools. The concentration ratio can be adjusted by modulating the reservoir volume and the number of Nafion coated channels, facilitating the application of this platform in rapid virus detection with enhanced sensitivity.

Acknowledgements

This work was supported by the Korea Ministry of Environment under the “Projects for Developing Eco-Innovation Technologies (GT-11-G-02-001-1)”, the Pioneer Research Center Program through the National Research Foundation of Korea funded by the Ministry of Science, ICT & Future Planning (2012-0009565), and the Human Resources Program in Energy Technology of the Korea Institute of Energy Technology Evaluation and Planning (KETEP) grant financial resource from the Ministry of Trade, Industry & Energy, Republic of Korea (no. 20124010203250).

Notes and references

- 1 D. S. Burgi and R. L. Chien, *Anal. Chem.*, 1991, **63**, 2042–2047.
- 2 H. Cui, K. Horiuchi, P. Dutta and C. F. Ivory, *Anal. Chem.*, 2005, **77**, 1303–1309.
- 3 B. Jung, R. Bharadwaj and J. G. Santiago, *Anal. Chem.*, 2006, **78**, 2319–2327.
- 4 S. Song, A. K. Singh and B. J. Kirby, *Anal. Chem.*, 2004, **76**, 4589–4592.
- 5 S. J. Kim, S. H. Ko, K. H. Kang and J. Han, *Nat. Nanotechnol.*, 2010, **5**, 297–301.
- 6 M. Kim, M. Jia and T. Kim, *Analyst*, 2013, **138**, 1370–1378.
- 7 S. H. Ko, Y.-A. Song, S. J. Kim, M. Kim, J. Han and K. H. Kang, *Lab Chip*, 2012, **12**, 4472–4482.
- 8 J. H. Lee and J. Han, *Microfluid. Nanofluid.*, 2010, **9**, 973–979.
- 9 W. H. Organization, 2002.
- 10 S. N. Peirson, J. N. Butler and R. G. Foster, *Nucleic Acids Res.*, 2003, **31**, e73–e73.
- 11 K. Hyoungh Kang, X. Xuan, Y. Kang and D. Li, *J. Appl. Phys.*, 2006, **99**, 064702.
- 12 H. Jeon, H. Lee, K. H. Kang and G. Lim, *Sci. Rep.*, 2013, **3**.
- 13 D. Di Carlo, *Lab Chip*, 2009, **9**, 3038–3046.
- 14 J. Fontanella, M. McLin, M. Wintersgill, J. Calame and S. Greenbaum, *Solid State Ionics*, 1993, **66**, 1–4.
- 15 R. J. Russell, P. S. Kerry, D. J. Stevens, D. A. Steinhauer, S. R. Martin, S. J. Gamblin and J. J. Skehel, *Proc. Natl. Acad. Sci. U. S. A.*, 2008, **105**, 17736–17741.
- 16 E. Fu, T. Liang, P. Spicar-Mihalic, J. Houghtaling, S. Ramachandran and P. Yager, *Anal. Chem.*, 2012, **84**, 4574–4579.